Published in final edited form as:
J Nat Prod. 2009 December ; 72(12): 2091–2097. doi:10.1021/np900334k.

Biologically Active Tetranorditerpenoids from the Fungus *Sclerotinia homoeocarpa*, Causal Agent of Dollar Spot in Turfgrass

H. M. T. Bandara Herath[†], **Wimal H. M. W. Herath**[†], **Paulo Carvalho**[⊥], **Shabana I. Khan**[†], **Babu L. Tekwani**[†], **Stephen O. Duke**[‡], **Maria Tomaso-Peterson**[§], and **N. P. Dhammika Nanayakkara**[†,*]

[†]National Center for Natural Products Research, Research Institute of Pharmaceutical Sciences, University of Mississippi, University, MS 38677

[⊥]Department of Medicinal Chemistry, School of Pharmacy, University of Mississippi, University, MS 38677

[‡]Natural Products Utilization Research Unit, USDA-ARS, University, MS 38677

[§]Department of Entomology and Plant Pathology, Mississippi State University, Mississippi State, MS 39762

Abstract

Nine new tetranorditerpenoid dilactones (**2–10**), together with two previously reported norditerpenoids dilactones (**1, 11**), and two known putative biosynthetic intermediates oidiolactone-E (**12**) and **13** were isolated from an ethyl acetate extract of a culture medium of *Sclerotinia homoeocarpa*. Structures and absolute configuration of these compounds were determined by spectroscopic methods and confirmed by X-ray crystallographic analysis of representative compounds. Compounds were evaluated for herbicidal, antiplasmodial and cytotoxic activities. Compounds **1, 2, 6, 7, 11** were more active as growth inhibitors in a duckweed bioassay (I_{50} values of 0.39 - 0.95 μM) than more than half of 26 commercial herbicides previously evaluated using the same bioassay. Some of these compounds exhibited strong antiplasmodial activities as well, but they also had cytotoxic activity thus precluding them as potential antimalarial agents.

Malaria continues to be a major cause of morbidity and mortality in many parts of the tropics and subtropics. Every year about 500 million people become ill with malaria and over a million people, most of them young children, die of this disease.[1] Wide-spread resistance to first-line antimalarial drugs has hampered the effective control of this disease. Many efforts are underway to develop new classes of antimalarials to counter this trend.[2] One of these involves searching for compounds to inhibit unique metabolic pathways in the apicoplast.[2,3]

Plasmodium parasites, which cause malaria in humans, contain an organelle called the apicoplast.[4] The apicoplast is very similar to plastids (chloroplasts are one of several plastid forms) of plants and is believed to have been acquired by the engulfment of an ancestral alga and retention of the algal plastid. The apicoplast is essential for the survival of parasites, and it contains many plant-like metabolic pathways such as essential amino acid, heme, and type

*To whom correspondence should be addressed. Tel.: 1-662-915-1019. Fax: 1-662-915-1006. dhammika@olemiss.edu .

II fatty acid biosynthesis not present in the vertebrate hosts of malaria parasites.[4] Several studies have been initiated to evaluate antimalarial activity of herbicides and natural phytotoxins which are known to inhibit metabolic pathways of the plastid in plants.[5–7]

A number of plant pathogenic fungi are known to release phytotoxins that disrupt biological processes in plants.[8–10] Some of these have also been shown to inhibit metabolic pathways in the plastid;[11] thus, plant pathogens could be a potential source of antimalarial compounds.

As part of a program to search for antimalarial compounds from natural sources, we initiated a project to screen phytopathogenic fungi for antimalarial activity. *Sclerotinia homoeocarpa* is the causal agent of "dollar spot," the most prevalent disease of turfgrass in North America.[12] Previous studies on *S. homoeocarpa* led to the isolation of two tetranorditerpene dilactones with potent phytotoxic activity.[13]

In preliminary studies, *S. homoeocarpa* was isolated from an infected grass leaf and was grown in potato/dextrose (PD) broth. The ethyl acetate extract of PD broth showed herbicidal activity, as well as in vitro antimalarial activity, against chloroquine sensitive (D-6) and chloroquine sensitive resistant (W-2) strains of *Plasmodium falciparum*. Chemical investigation of this extract led to the isolation of eleven tetranorditerpene dilactones and two putative biogenetic precursors with partially and fully opened lactones.

A number of compounds of this class have been previously isolated from fungi.[13–20] These compounds were very similar to podolactones from the plant family Podocarpaceae.[21] Norditerpene dilactones have shown herbicidal,[13,15,19,22,23] antitumor,[20] antifungal,[15,17,24,25] insecticidal,[27] anti-feedant,[28,29] and cytokine production inhibitory activities.[14]

Nine compounds (**2–10**) isolated in the present study, all norditerpenoid dilactones, have not been previously reported. Compound **1** had been identified from an isolate of *S. homoeocarpa* from Japan, and its herbicidal activity was described.[13] Spectroscopic data of compound **9** resembled those of a previously reported compound to which a different structure was assigned.[19,30] Compound **11** was first reported by synthesis[30] and was later isolated from an unidentified fungus.[20] Compound **12** and **13** were reported from *Oidiodendron truncata* [14] and from an *Acrostalagmus* species,[18] respectively. Most of the compounds described herein showed both phytotoxic and antiplasmodial activity; however, they also had a relatively high level of general cytotoxcity.

Results and Discussion

Spectroscopic data indicated that a majority of the compounds isolated from *S. homoeocarpa* belong to the teteranorditerpene dilactone class.[15,25,30] The molecular weight of compound **1** was determined to be $C_{16}H_{16}O_6$ by HRESIMS. The NMR data of **1** agreed well with those reported for N-1400A, which was previously isolated from an isolate of *S. homoeocarpa*.[13] Since the assignments of ^1H and ^{13}C NMR data for N-1400A were not previously reported, they are presented in Tables 1 and 2. The relative configuration of this compound was also determined for the first time. The ROESY spectrum of compound **1** showed correlations of CH_3- 15 to H-3, H-5, and H-6, indicating that they are on the same face. However, the absence of any ROESY correlation of CH_3-16 prevented assignment of the relative configuration of all the asymmetric centers of this compound by spectroscopic methods. X-ray crystallography (Figure 1) was used to establish the relative configuration of all the asymmetric centers.

The molecular formula of compound 2 was determined to be $C_{16}H_{16}O_5$ by HRESIMS. Comparison of ^1H NMR spectra of compounds **2** and **1** indicated that the signal due to the oxygenated methine at C-3 of the latter had been replaced by up-field signals at 2.23 and

2.79 in the former. Comparison of the ^{13}C NMR spectra of **2** and **1** showed the replacement of the signal due to C-3 (δ 69.4) of the latter by an up-field signal at δ 31.8 in the former, and also up-field shifts of the carbon signals that were β and γ to C-3. These observations suggested that compound **2** was the 3-dehydroxy analog of **1. HMBC** correlations between C-3 methylene signals (δ 2.23 and 2.79) and C-1 (δ 128.7), C-2 (δ 127.7), C-4 (δ 43.0), C-5 (δ 45.0), C-14 (δ 181.6), and C-15 (δ 25.0) supported this structure. The COSY, HMQC, and HMBC correlations of the rest of the molecule were similar to those observed for compound **1**, further confirming this structure for compound **2**. ROESY correlations of CH_3-15 to H-5, H-6 indicated that they were on the same face, and correlations of CH_3-16 to H-7 showed that they were on the opposite face. These results established that **2** had the same relative configuration as compound **1**.

HRESIMS data indicated the molecular formula $C_{16}H_{18}O_6$ for compound **3**. The ^{1}H NMR and ^{13}C NMR spectra of **3** were also similar to those of compound **1**, except for signals due to protons in ring A. The major difference was the replacement of signals due to two olefinic protons by two methylene groups [2H-1: δ 1.68 (m), and 1.93 (m), 2H-2: δ 1.75 (m), and 1.89 (m)]. Correlations in the COSY spectrum showed that these two methylene groups were attached to an oxygenated methine (δ 4.25) to form a -CH_2CH_2CHOH- moiety. Although no HMBC cross-peaks were observed between the oxygenated methine proton at δ 4.25 and any carbon, strong correlations between 15-CH_3 (δ 1.30) and the carbon signal of this methine (δ 65.7), in addition to C-2 (δ 26.7), C-4 (δ 48.1), C-5 (δ 43.5), and C-14 (δ 181.2) indicated that it was located at C-3. This observation, in combination with the molecular formula, suggested that **3** was the 1,2-dihydro- analog of **1**. Additional HMBC correlations from 2H-1 (δ 1.68 and 1.93) to C-2 (δ 26.7), C-3 (δ 65.7), C-5 (δ 43.5), C-9 (δ 159.0), C-10 (δ 35.6), and C-16 (δ 27.2), as well as 2H-2 (δ 1.75 and 1.89) to C-1 (δ 27.7), C-3 (δ 65.7), C-4 (δ 48.1), and C-10 (δ 35.6) were supportive of this structure. The HMBC correlations of the rest of the molecule were identical to those of **1**. The coupling constants of H-3 (J = 8.8, 3.2 Hz) indicated that it was axial. When the OH group at C-3 is equatorial it shows a strong interaction with the 15-CH_3 group. This was evident from the significant up-field shift of the ^{13}C signal (δ 15.9) compared to that of compounds **2**, or **1** (δ 24.5 and δ 25.0, respectively). ROESY correlation of CH_3-16 to H-3 and H-7 showed that they were on the same face, β. ROESY correlations of 15-CH_3 to H-5 and H-6 indicated that the relative configurations at C-4, C-5, C-6, C-7, C-8, and C-10 were similar to those assigned for compound **1**. An X-ray crystallography study of **3** (Figure 1) confirmed the structure and the relative configuration of compound **3**.

The molecular formula of compound **4**, $C_{16}H_{18}O_6$, determined by HRESIMS, was the same as that of **3**. Comparison of ^{1}H NMR spectra of these two compounds indicated that the only difference was the position of the OH group in the A ring. In the COSY spectrum, the oxygenated methine at δ 3.96 showed strong cross-peaks to H-1 (δ 1.51 and 2.32) and H-3 (δ 1.86 and 2.05), indicating that the OH group was at on C-2. HMBC correlations were not observed between H-2 and adjacent carbons; however, correlations of H-1 to C-2, C-3, C-5, C-9, C-10, and C-16; and H-3 to C-1, C-2, C-4, C-5, C-14, and C-15 confirmed this structure. COSY and HMBC correlations for the rest of the molecule were identical to those observed for compound **1**. Even though the 2-hydoxylated methine appeared as a broad multiplet, coupling constants of H-1 and H-3 clearly indicated that H-2 was axial. ROESY correlation of H-2 to H-5 and CH3-15 indicated that it was in α oriented. The rest of the ROESY correlations of **4** were similar to those observed for **1**, suggesting that the relative configurations of the remaining asymmetric centers were the same as those of the latter.

Compound **5** was determined to have the same molecular formula ($C_{16}H_{18}O_6$), as those of compounds **3** and **4**. Comparison of ^{1}H NMR and ^{13}C NMR spectra of **3–5** indicated that **5** only differed in the position of the OH group on the A ring. The COSY spectrum displayed

a spin system consisting of two adjacent methylene groups connected to a hydroxyl methine [δ 3.94 (t, *J* = 6.0 Hz)]. Since the 3-OH analog had been identified, the OH group had to be on C-1. HMBC correlations of H-1 to C-2, C-3, C-5, C-9, C-10, and C-16 confirmed its location. The other HMBC correlations were very similar to those observed for compound **1**. The coupling constant of H-1 (t, *J* = 6.0 Hz) indicated that it was in equatorial configuration. An axial OH group on C-1 would lead to interaction between this group and the CH_3-16 group. This was evident from the up-field shift of C-16 (δ 17.8) compared to that of compounds **3** and **4** (δ 27.2 and 29.1, respectively). In the ROESY spectrum, correlations of H-5 to H-1, H-6, and CH_3-15 indicated that they were on the same face, α. All of these data suggested the structure and relative configuration depicted for compound **5**.

The molecular formula of compound **6** was determined to be $C_{16}H_{16}O_5$; one oxygen less than that observed for compound **1**. Comparison of the NMR spectra of compounds **6** and **1** indicated close similarities in the signals of the A ring. The differences of the remaining signals could be attributed to the replacement of the epoxy group in the B ring of the latter by a double bond in the former. The COSY spectrum showed, in addition to the ABX spin system due to H- 1, H-2 and H-3 as observed in compound **1**, a second system due to H-5 (δ 2.29, d, *J* = 5.2 Hz), H-6 (δ 5.01, t, *J* = 5.0 Hz), H-7 (δ 6.24, m), H-11 (δ 6.00, d, *J* = 1.6 Hz), and H-13 [δ 4.91 (d, *J* = 13.6 Hz) δ 5.01 (dt, *J* = 13.6, 2.0 Hz)]. In the HMBC spectrum, the olefinic proton H-1 (δ 6.61) showed correlations to the carbons C-3, C-9, C-5, and C-10 and H-3 (δ 4.42) to C-1, C-2, C-4, C-5, C-14, and C-15. Additionally, H-6 showed correlations to C-5, C-7, C-8, C-10; H-7 to C-5, C-9 and C-13; H-11 to C-8, C-10, C-12, and C-16; H-13 to C-7, C-8, C-9, and C-12. The ROESY spectrum showed correlations of H-3 to H-5 and H-5 to H-6, indicating that all these protons were on the same face; however, due to the close proximity of ^{1}H signals of CH_3-15 and CH_3-16, the ROESY spectrum was of limited use to determine the relative configuration of all asymmetric centers of this compound. An X-ray crystallographic study of this compound (Figure 1) confirmed the structure and relative configuration of **6** as depicted.

The molecular formula of compound **7** was confirmed to be $C_{16}H_{16}O_4$ by HRESIMS. Comparison of the ^{1}H- and ^{13}C NMR spectra showed that 7 was the 3-dehydroxy analog of compound **6** (see Tables 1 and 2). The COSY spectrum showed the presence of a -CH=CHCH_2- spin system very similar to that observed for compound **2**. The HMBC spectrum correlations ofH-3 (δ 2.26, 2.83) to C-1, C-2, C-4, C-5, C-14, and C-15 confirmed that the methylene was at 3. The other HMBC correlations were similar to those observed for compound **6**. The ROESY spectrum showed correlations between CH_3-15 and H-5, H-6 as well as to one of the H-3 (δ 2.26) protons, suggesting that they are on the same face. On the other hand, CH_3-16 showed a correlation to the other H-3 (δ 2.83) protons, indicating that they are on the opposite phase. The data indicated that the relative configurations of the asymmetric centers of compound **7** were the same as those observed for compound **6**.

HRESIMS data suggested molecular formula C16H18O5 for compound **8**. ^{1}H NMR and ^{13}C NMR data of this compound and compound **6** were similar except for the signals in ring A. The differences were due to replacement of the double bond in the A ring in **6** by two methylene groups in **8**. This information indicated that **8** was the 1,2-dihydro analog of **6**. The COSY spectrum showed the presence of a -CH_2CH_2CHOH- spin system, very similar to that observed for compound **3**. HMBC correlations of H-3 (δ 4.31) to C-1, C-2, C-14, and C-15, and H-1 (δ 1.66 and 1.83) to C-2, C-3, C-5, and C-16 further supported this structure. The other correlations were very similar to those observed for compound **6**. Coupling constants of H-3 (dd, *J* = 11.2, 4.0 Hz) indicated that it was axial. As in the case of compound **3**, the chemical shift of C-15 (δ, 15.9) in **8** had shifted up-field relative to that of **6** and **7** (δ 25.0, 25.4, respectively), probably due to its interaction with the equatorial 3-OH group. The ROESY spectrum showed correlations between CH_3-15 and H-5, H-6,

suggesting that they were on the same face, α. The ROESY correlation of CH_3-16 to H-3 indicated that they were on the same face, β. The 3-epimer of **8** was synthesized previously.[30]

Compound **9** had molecular formula, $C_{16}H_{18}O_5$ (HRESIMS), identical to that of **8**. Comparison of ^{1}H NMR spectra showed that signals in the ring A of compounds **9** and **4** and signals in rings B and C of compounds **9** and **8** were superimposable. This suggested that compound **9** was the 2-OH isomer of **8**. As in the case of compound **4**, no HMBC correlations were observed between H-2 and adjacent carbons in compound **9**. However, correlations of 2H-1 (δ 1.34, 2.20) to C-2, C-3, C-5, C-9, C10, and C-16, and 2H-3 (δ 1.68, 1.96) to C-1, C-2, C-4, C- 5, C-14, and C-15 confirmed this structure. The other HMBC correlations were identical to those observed for **8**. On the basis of coupling constants, the 2-OH group was determined to be equatorial. Relative configuration of **9** was determined by ROESY.

Barrero et al.[30] previously revised the structure of wentilactone B[19] to the 2-epimer of **9**. Although the ^{1}H NMR data observed for **9** were different from those reported for wentilactone B by Dorner et al.,[19] data reported for the same compound by Barrero et al.[30] had close resemblance if the assignments for H-1 and H-3 were interchanged. There is a possibility that wentilactone is the 2β-hydroxy analog and is not the 2α-hydroxy analog proposed by Barreiro et al. [30] by comparison with the data reported for 2α-hydroxynagilactone[31] In light of the current study, the conformation of the 2-OH group of both should be revised to β. The complete assignment of NMR data were not previously reported for wentilactone B[19]; thus, the data for **9** were included in Tables 1 and 2.

The molecular formula of compound **10** ($C_{16}H_{18}O_5$) was identical to those of $_8$ and $_9$. Comparison of $_1$H NMR showed that signals in the A rings of compound **10** were superimposable with those of compound **5**, and signals of the B and C rings of **10** exhibited strong similarities to those of compounds **8** and **9** except for a down-field shift of H-11, possibly due to interaction of H-11 with the 1β-hydroxy group. This indicated that **10** was the 1β-hydroxy isomer of **8**. A similar shift of the H-11 signal was also observed for compound **5**, relative to those of **3** and **4**. HMBC correlations of H-1 (δ 3.78) to C-3, C-9, C-10, and C16 and H-3(δ 1.38, 1.13) to C-1, C-2, C-4, C-5, C-14, and C-15 confirmed the structure. The coupling constant of 1-H (t, J = 6.4 Hz) showed that it was equatorial. An axial OH group on C-1 resulted in an up-field shift of the CH_3-16 signal relative to those in **9** and **8**, similar to that observed for compound **5** relative to **3** and **4**. In the ROESY spectrum, correlations of CH_3-15 to H-5 and H-6, and H-5 to H-6 and H-1 suggested that they were on the same face, α. An X-ray crystallographic analysis of **10** (Figure 1) confirmed the structure and the relative configuration as shown.

Compounds **11**,[20,32] **12**,[15] and **13**,[18] were identified by comparing physical and spectral data with those reported in the literature.

The absolute configuration of the compounds was determined by comparing CD curves with those previously reported for this class of compounds.[17,19,25] Compounds **1–5** showed negative Cotton effects at 265–270 nm in CD curves indicating that the absolute configuration at common asymmetric centers was 4*S*, 5*R*, 6*S*, 7*R*, 8*R*, 10*S* as depicted. Similarly, compounds **6– 11** showed negative Cotton effects at 290–296 nm in CD curves indicating that the absolute configuration at common asymmetric centers was 4*S*, 5*R*, 6*S*, 10*S* as depicted.

The in vitro antiplasmodial activities of compounds **1–13** are summarized in Table 3. Compounds **6** (IC_{50} 43 and 32 ng/mL), **9** (IC_{50} 97 and 84 ng/mL) and 7 (IC_{50} 170 and 130 ng/mL) demonstrated strong antiplasmodial activities whereas compounds **3, 5, 8** and **13**

were inactive. Selectivity index of antiplasmodial activity was calculated based on their cytotoxicity to mammalian kidney fibroblasts (Vero cells) determined in parallel experiments. All of the compounds with strong antiplasmodial activities also were cytotoxic to Vero cells, and their low selectivity indices (<30) preclude them as antimalarial drug candidates. The cytotoxic potential of these compounds was also evaluated against a panel of solid tumor cell lines and kidney epithelial cells (Table 4). The order of cytotoxic activity was similar in all cell lines for most ofthe compounds, and was parallel to their antiplasmodial activity. These observations suggested that the antiplasmodial activity of these compounds was a manifestation of their general cytotoxicity. The presence of a lactone in ring C appeared to be essential for the activity of these compounds.

Compounds **1, 2, 4–7, 9–11** showed total growth inhibition of a dicot (lettuce: *Lactuca sativa* cv. L. Iceberg) and a monocot (bentgrass: *Agrostis stolonifera*) at concentrations of 1 mg/mL and 0.1 mg/mL and partial inhibition at 0.001 mg/mL (Table 6). Compounds **3** and **8** caused total inhibition of growth only at the highest concentration (1 mg/mL). Compound **12** showed moderate activity at the highest concentration, and compound **13** was inactive. It appears that the lactone in ring C is essential for the phytotoxicity. However, this activity did not strongly correlate with the cytotoxic activity.

More detailed evaluation of the herbicidal activity of compounds **1, 2, 4–7, 9–11** was made in a duckweed (*Lemna pausicostata*) bioassay that evaluates growth after exposure to different concentrations of the compounds (Figure 2). The most active compounds (**1, 2, 6, 7, 11**) were more active than more than half of 26 commercial herbicides using exactly the same bioassay under identical conditions in the same laboratory.[33] The I_{50} value for 1 (0.39 μM) was lower than 19 of the commercial herbicides previously tested with this assay. Macías et al.[22] and Barrero et al.23 reported **11** to be a potent phytotoxin on a number of plant species. Dorner et al.[19] found **9** to be a weak inhibitor of wheat coleoptile elongation. However, this assay is not valid for most herbicides. Using a duckweed assay similar to ours, John et al.[15] reported two compounds, structurally related to ours, to be “strongly herbicidal.” A Japanese patent[13] exists on herbicidal activity of this class of compounds. Compounds **1** and **3** have been included in its claims for as herbicides although the latter has not been identified.[13]

Experimental Section

General Experimental Procedures

Melting points were measured in a Uni-melt, Thomas Hoover capillary melting point apparatus. NMR spectra were recorded on a Bruker 400 MHz spectrometer using $CDCl_3$/CD_3OD (1:1) as the solvent unless otherwise stated. MS analyses were performed on an Agilent Series 1100 SL equipped with an ESI source (Agilent Technologies, Palo Alto, CA, USA). All acquisitions were performed under positive ionization mode. Column chromatography was carried out on Merck silica gel 60 (230–400 mesh). Preparative TLC was carried out using silica gel GF plates (20 × 20 cm, thickness 0.25 mm).

Isolation of *Sclerotinia homoeocarpa*

Sclerotinia homoeocarpa F.T. Bennett was isolated from an infected grass blade collected near the Sardis Lake dam site, Sardis, Mississippi and identified by Dr. Maria Tomaso-Peterson, of the Department of Entomology and Plant Pathology, Mississippi State University, Mississippi State. A voucher specimen (DN5-59-1) was deposited in the fungal collection at the National Center for Natural Products Research, University of Mississippi.

Extraction and Purification

S. homoeocarpa cultures, in 40 conical flasks (1 L) containing 600 mL of potato/dextrose liquid medium, were incubated for 21 days at 27 °C on an orbital shaker at 125 rpm. The medium was separated by filtration and extracted three times with ethyl acetate. The EtOAc extract was evaporated to dryness, and the crude extract (3.31 g) was thoroughly washed with hexanes. The hexanes insoluble dark brown gum (2.24 g) was chromatographed on silica gel. The column was eluted sequentially with hexanes/CH_2Cl_2 and CH_2Cl_2/MeOH with increasing concentrations of MeOH, collecting 500 mL volumes to give eight major fractions, F-1 (hexanes:CH_2Cl_2, 4:1, 170 mg), F-2 (hexanes:CH_2Cl_2, 1:1, 147 mg), F-Page3 (hexanes:CH_2Cl_2, 3:4, 370 mg), F-4 (CH_2C_{l2}, 247 mg), F-5 (CH_2Cl_2:MeOH, 99:1, 285 mg), F-6 (CH_2C_{l2}:MeOH, 98:2, 214 mg), F-7 (CH_2Cl_2:MeOH, 95:5, 154 mg) and F-8 (CH_2Cl_2:MeOH, 90:10, 228 mg). Fractions, F-3, F-4 and F-5 showed significant antiplasmodial activities. Separation of F-3 by PTLC (CH_2Cl_2:MeOH, 97.5:2.5) afforded compounds **1** (123 mg) and **6** (224 mg) and a mixture, which was further separated by PTLC (hexanes:EtOAc, 7:3) to afford **4** (23 mg) and **9** (15 mg). Similarly, separation of F-4 by PTLC (hexanes:EtOAc, 60:40 × 2) gave compounds **2** (34 mg), **7** (37 mg), **11** (39 mg), and impure **3** (5 mg) which was further purified by PTLC (CH_2Cl_2:MeOH, 98:2). Separation of F-5 by PTLC (hexanes:EtOAc, 60:40 × 2) afforded compounds **5** (67 mg) and **8** (12 mg) and a mixture, which was further separated (PTLC, CH_2Cl_2:MeOH, 95:5) to give **10** (10 mg) and **12** (82 mg). Re-crystallization of the white solid precipitated from F-8 (CH_2Cl_2 / MeOH) afforded compound **13** (87 mg).

Compound 1—colorless needles (CH_2C_{l2}/hexane); mp 258–259 °C; $[\alpha]^{26}_{D}$ +2.1 (*c* 0.67, $CHCl_3$:CH_3OH 9:1); UV (CH_3OH) λ_{max} (log ε) 218 (4.12); CD (CH_3OH) $[\theta]_{267}$ -21.6; ^1H NMR and ^{13}C NMR data (see Tables 1 and 2); HRESIMS $[M + H]^+$ *m/z* 305.1041 (calcd for $C^{16}H^{17}O^6$, 305.1025).

Compound 2—colorless needles (CH_2Cl_2/hexane); mp 160–162 °C; $[\alpha]^{26}_{D}$ -54.0 (*c* 0.43, $CHCl_3$:CH_3OH 9:1); UV (CH_3OH) λ_{max} (log ε) 216 (4.08); CD (CH_3OH) [θ]265 -20.6; ^1H NMR ($CDCl_3$) and ^{13}C NMR data (see Tables 1 and 2); HRESIMS $[M + H]^+$ *m/z* 289.1094 (calcd for $C_{16}H_{17}O_5$, 289.1076)

Compound 3—colorless needles (EtOAc/hexane); mp 260–261 °C; $[\alpha]^{26}_{D}$ +34.3 (*c* 0.30, $CHCl_3$); UV (CH_3OH) λ_{max} (log ε) 215 (4.10); CD (CH_3OH) $[\theta]_{265}$ -21.8; ^1H NMR and ^{13}C NMR data (see Tables 1 and 2); HRESIMS $[M + H]^+$ *m/z* 307.1207 (calcd for $C_{16}H_{19}O_6$, 307.1182).

Compound 4—colorless needles (MeOH/CH_2Cl_2); mp 248–250 °C; $[\alpha]^{26}_{D}$ +30.6 (*c* 0.63, $CHCl_3$:CH_3OH 9:1); UV (CH_3OH) λ_{max} (log ε) 219 (4.2); CD (CH_3OH) $[\theta]_{270}$ -19.4; ^1H NMR and ^{13}C NMR data (see Tables 1 and 2); HRESIMS $[M + H]^+$ *m/z* 307.1193 (calcd for $C_{16}H_{19}O_6$, 307.1182).

Compound 5—colorless needles (EtOAc/hexane); mp 240–241 °C; $[\alpha]^{26}_{D}$ -46.2 (*c* 0.28, $CHCl_3$); UV (CH_3OH) λ_{max} (log ε) 215 (4.33); CD (CH_3OH) [θ]265 -35.0; ^1H NMR and ^{13}C NMR data (see Tables 1 and 2); HRESIMS $[M + H]^+$ *m/z* 307.1176 (calcd for $C_{16}H_{19}O_6$, 307.1182).

Compound 6—colorless prisms (MeOH); mp. 252–253 °C; $[\alpha]^{26}_{D}$ +262.2 (*c* 0.57, $CHCl_3$:CH_3OH 9:1); UV (CH_3OH) λ_{max} (log ε) 260 (4.26); CD (CH_3OH) $[\theta]_{295}$ -5.0; ^1H NMR and ^{13}C NMR data (see Tables 1 and 2); HRESIMS $[M + H]^+$ *m/z* 289.1095 (calcd for $C_{16}H_{17}O_5$, 289.1076).

Compound 7—colorless needles (CH_2Cl_2/hexane); mp 160–162 °C; [α] $^{26}_{D}$ -162.0 (*c* 0.52, $CHCl_3$:CH_3OH 9:1); UV (CH_3OH) λ_{max} (log ε) 260 (4.18); CD (CH_3OH) $[\theta]_{292}$ -12.3; ^{1}H NMR ($CDCl_3$) and ^{13}C NMR data (see Tables 1 and 2); HRESIMS $[M + H]^+$ *m/z* 273.1149 (calcd for $C_{16}H_{17}O_4$, 273.1127).

Compound 8—colorless needles (CH_2Cl_2/hexane); mp 244–245 °C; [α] $^{26}_{D}$ -180.1 (*c* 0.63, $CHCl_3$:CH_3OH 9:1); UV (CH_3OH) λ_{max} (log ε) 260 (4.40); CD (CH_3OH) $[\theta]_{290}$ -24.7; ^{1}H NMR and ^{13}C NMR data (see Tables 1 and 2); HRESIMS $[M + H]^+$ *m/z* 291.1249 (calcd for $C_{16}H_{19}O_5$, 291.1232).

Compound 9—colorless needles ($CHCl_3$/hexane); mp 254–256 °C; [α] $^{26}_{D}$ -236.5 (*c* 0.58, $CHCl_3$:CH_3OH 9:1); UV (CH_3OH) λ_{max} (log ε) 260 (4.3); CD (CH_3OH) $[\theta]_{295}$ -3.9; ^{1}H NMR and ^{13}C NMR data (see Tables 1 and 2); HRESIMS $[M + H]^+$ *m/z* 291.1251 (calcd for $C_{16}H_{19}O_5$, 291.1232).

Compound 10—colorless needles ($CHCl_3$/hexane); mp 235–236 °C; [α] $^{26}_{D}$ -56.3 (*c* 0.33, $CHCl_3$); UV (CH_3OH) λ_{max} (log ε) 260 (4.21); CD (CH_3OH) $[\theta]_{288}$ -26.1; ^{1}H NMR and ^{13}C NMR data (see Tables 1 and 2); HRESIMS $[M + H]^+$ *m/z* 291.1249 (calcd for $C_{16}H_{19}O_5$, 291.1232).

Compound 11—colorless needles ($CHCl_3$/hexane); mp 194–195 °C (lit 191–193 °C);[32] [α]26 $_{D}$ -272.1 (*c* 0.53, $CHCl_3$:CH_3OH 9:1) (lit. −332.7);[32] UV (CH_3OH) λ_{max} (log ε) 260 (4.21); CD (CH_3OH) $[\theta]_{296}$ -5.1.

Compound 12—colorless needles ($CHCl_3$/hexane); mp 240−241 °C (lit. 237 °C);[15] [α]26 $_{D}$ - 33.4 (*c* 0.36, $CHCl_3$:CH_3OH 9:1) (lit. −38.5).[15]

Compound 13—colorless needles ($CHCl_3$/hexane); mp 214–216 °C (lit 200 °C);[18] [α]26 $_{D}$ +27.8 (*c* 0.36, $CHCl_3$:CH_3OH 9:1) (lit. +22.5).[18]

Crystallographic Data for Compounds 1, 3, 6, and 10

All single crystal X-Ray diffraction data were collected on a Bruker Smart Apex II system, using Cu Kα radiation with a graphite monochromator, fine-focus sealed tube. The crystal was kept at 100 K under a stream of cooled nitrogen gas from a KRYO-FLEX low temperature device. Data collection, indexing and initial cell refinements were all carried out using APEX II software. Frame integration and final cell refinements were done using SAINT software. Structure solution, refinement, graphics and generation of publication materials were performed using SHELXTL, V6.12 software. Hydrogen atoms were placed their expected chemical positions using the HFIX command and were included in the final cycles of least squares with isotropic Uij‘s related to the atom’s ridden upon.

Compound 1—$C_{16}H_{16}O_6$, MW = 304.29, orthorhombic space group $P2_12_12_1$, a = 6.5821 (4) Å, b = 11.0090 (7) Å, c = 18.2832 (12) Å, α = β = γ = 90°, V = 1324.84 (15) Å^3, Z=3, crystal dimensions 0.23 × 0.18 × 0.14 mm. The final cell parameters were determined from least-squares refinement on 6799 reflections, with R*int* = 0.058, and *wR*(F^2) = 0.076. The supplementary crystallographic data can be obtained free of charge from The Cambridge Crystallographic Data Centre, reference number CCDC 681270, via www.ccdc.cam.ac.uk/data_request/cif.

Compound 3—$C_{16}H_{18}O_6$, *MW* = 306.30, orthorhombic space group $P2_12_12_1$, *a* = 7.7869 (2) Å, *b* = 9.1234 (3) Å, *c* = 19.6990 (6) Å, α = β = γ = 90°, *V* = 1399.48 (7) Å^3, Z=4, crystal dimensions 0.26 × 0.23 × 0.11 mm. The final cell parameters were determined from least-

squares refinement on 5987 reflections, with *R*int = 0.031, *and wR*(F^2) = 0.069. The supplementary crystallographic data can be obtained free of charge from The Cambridge Crystallographic Data Centre, reference number CCDC 681271, via www.ccdc.cam.ac.uk/data_request/cif.

Compound 6—$C_{16}H_{15}O_5$, *MW* = 288.30, or space group $P2_12_12_1$, *a* = 6.29910 (10) Å, *b* = 6.55110 (10) Å, *c* = 32.5925 (6) Å, α = β = γ = 90°, *V* = 1344.96 (4) $Å^3$, Z=4, crystal dimensions 0.28 × 0.22 × 0.14 mm. The final cell parameters were determined from least-squares refinement on 7789 reflections, with *R*int =0.022, *and wR*(F^2) =0.070. The supplementary crystallographic data can be obtained free of charge from The Cambridge Crystallographic Data Centre, reference number CCDC 681272, via www.ccdc.cam.ac.uk/data_request/cif.

Compound 10—$C_{16}H_{18}O_5$, *MW* = 290.30, monoclinic space group $P2_1$, *a* = 6.1595 (2) Å, *b* = 14.2378 (5) Å, *c* = 8.3456 (3) Å, α = γ = 90°, β = 107.479 (2)°, *V* = 698.10 (4) $Å^3$, Z=2, crystal, dimensions 0.21 × 0.14 × 0.08 mm. The final cell parameters were determined from least-squares refinement on 3166 reflections, with *R*int =0.017, *and wR*(F^2) =0.071. The supplementary crystallographic data can be obtained free of charge from The Cambridge Crystallographic Data Centre, reference number CCDC 681273, via www.ccdc.cam.ac.uk/data_request/cif.

Phytotoxicity Assays

Initial phytotoxicity bioassays were carried out according to the procedure previously described by Dayan et al.,[34] using bentgrass (*Agrostis stolonifera*) and lettuce (*Lactuca sativa* cv. L. Iceberg), in 24-well plates. Test compounds (1 mg each) were dissolved in 100 µL of 5% CH_3OH in $CHCl_3$ and a 20 µL aliquot of each solution was pipetted onto the filter paper and dried for 30 minutes by airflow in a sterile biohazard hood. Water (200 µl) was added after placing the dried and sample impregnated filter paper in the well. The solvent controls were treated identically, using the solvent described above. Phytotoxicity was ranked visually. The ranking of phytotoxic activity was based on a scale of 0 to 5; 0 no effect; 5 no growth.

Further bioassays were conducted with the most active compounds from the initial bioassay using duckweed (*Lemna pausicostata*).[33] Plants were incubated with growth medium (pH 6.4) in a conical flask. Plants were grown autotrophically for a week in a growth chamber in continuous illumination (105 µmol $m^{-2}s^{-1}$) at 25±2°C. Fifty colonies of duckweed from the incubation colony were placed in 6-cm diam. polystyrene Petri dishes with 5 mL of nutrient medium containing test compound and 0.33 % stock solution solvent (5% v/v CH_3OH in CH_2Cl_2). This level of stock solution solvent had no effect on duckweed growth. Treatments for each dose were triplicated. Data were analyzed to determine I_{50} values using R software.[35]

Assay for *in vitro* Antiplasmodial (Potential Antimalarial) Activity

In vitro antiplasmodial activity was determined against D6 (chloroquin sensitive) and W2 (chloroquin resistant) strains of *P. falciparum* as described earlier.[36] A 200 µL suspension of red blood cells, infected with *P. falciparum* (2% parasitemia and 2% hematocrit), in RPMI 1640 mediumsupplemented with 10% human serum and 60 µg/mL Amikacin was added to the wells of a 96- well plate containing 10 µL of serially diluted samples. The plate was flushed with a gas mixture of 90% N_2, 5% O_2, and 5% CO_2 and incubated at 37 °C for 72 h in a modular incubation chamber (Billups-Rothenberg, CA). Parasitic LDH activity was determined by mixing 20 µL of the incubation mixture with 100 µL of Malstat™ reagent (Flow Inc., Portland, OR) and incubating at room temperature for 30 min. Then 20 µL of a

1:1 mixture of NBT/PES (Sigma, St. Louis, MO) was added, and the plate further incubated in the dark for 1 h. The reaction was then stopped by adding 100 μL of acetic acid (5%). Plates were read at 650 nm. Artemisinin and chloroquine were included in each assay as the drug controls, and IC_{50} values were computed from the dose response curves.

Assay for Cytotoxicity to Mammalian Cells

In vitro cytotoxicity was determined against a panel of mammalian cells that included kidney fibroblast (Vero), kidney epithelial (LLC-PK_{11}), malignant melanoma (SK-MEL), oral epidermal carcinoma (KB), breast ductal carcinoma (BT-549) and ovary carcinoma (SK-OV-3) cells.[37] The assays were performed in 96- well tissue culture-treated plates. Cells were seeded to the wells of 96-well plate at a density of 25,000 cells/well and incubated for 24 h. Samples at different concentrations were added and plates were again incubated for 48 h. The number of viable cells was determined by using Neutral Red dye, and IC_{50} values were obtained from dose response curves. Doxorubicin was used as a positive control.

Supplementary Material

Refer to Web version on PubMed Central for supplementary material.

Acknowledgments

This work was supported by the National Institute of Health (R21 A1061431-01) and in part by the United States Department of Agriculture, ARS, Specific Cooperative Agreement No. 58-6408-2-009. The authors sincerely thank Dr. Bharathi Avula, NCNPR, University of Mississippi, for recording the mass spectra, and Bob Johnson, NPURU, USDA-ARS, for his technical assistance in this research. Approved for publication as Journal Article No. J-11309 of the Mississippi Agricultural and Forestry Experiment Station, Mississippi State University.

References and Notes

1. World Malaria Report 2005. World Health Organization: Geneva; 2005.
2. Fidock DA, Rosenthal PJ, Croft SL, Brun R, Nwaka S. Nat. Rev. Drug Discovery 2004;3:509–520.
3. Ralph SA, D'Ombrain MC, McFadden GI. Drug Resistance Updates 2001;4:145–151. [PubMed: 11768328]
4. Waller RF, McFadden GI. Curr. Issues Mol. Biol 2005;7:57–80. [PubMed: 15580780]
5. Roberts F, Roberts CW, Johnson JJ, Kyle DE, Krell T, Coggins JR, Coombs GH, Milhous WK, Tzipori S, Ferguson DJP, Chakrabarti D, McLeod R. Nature 1998;393:801–805. [PubMed: 9655396]
6. Lichtenthaler HK. Biochem. Soc. Trans 2000;28:785–789. [PubMed: 11171208]
7. Bajsa J, Singh K, Nanayakkara D, Duke SO, Rimando AM, Evidente A, Tekwani BL. Biol. Pharm. Bull 2007;30:1740–1744. [PubMed: 17827731]
8. Hoagland RE. ACS Symposium Series 1990;439:2–52.
9. Evidente A. ACS Symposium Series 2006;927:62–75.
10. Strange RN. Nat. Prod. Rep 2007;24:127–144. [PubMed: 17268610]
11. Duke SO, Dayan FE. RIKEN Rev 1999;21:9–10.
12. Couch, HB. Diseases of Turfgrasses. 3rd ed. Malabar, Florida: Krieger Publishing Company; 1995. p. 65-69.
13. Yoneyama K, Tomie T, Tagawa M. Jpn. Kokai Tokkyo Koho. 2000 JP 2000247979 A 20000912.
14. Ichikawa K, Hirai H, Ishiguro M, Kambara T, Kato Y, Kim YJ, Kojima Y, Matsunaga Y, Nishida H, Shiomi Y, Yoshikawa N, Huang LH, Kojima N. J. Antibiot 2001;54:697–702. [PubMed: 11714224]
15. John M, Krohn K, Floerke U, Aust H-J, Draeger S, Schulz B. J. Nat. Prod 1999;62:1218–1221. [PubMed: 10514300]

16. Van Eijk GW, Roeijmans HJ, Van der AAHA. Antonie van Leeuwenhoek 1988;54:325–230. [PubMed: 3178188]
17. Ellestad GA, Evans RH Jr, Kunstmann MP, Lancaster JE, Morton GO. J. Am. Chem. Soc 1970;92:5483–5489. [PubMed: 5465204]
18. Ellestad GA, Evans RH Jr, Kunstmann MP. Tetrahedron Lett 1971:497–500.
19. Dorner JW, Cole RJ, Springer JP, Cox RH, Cutler H, Wicklow DT. Phytochemistry 1980;19:1157–1161.
20. Pettit GR, Tan R, Herald DL, Hamblin J, Pettit RK. J. Nat. Prod 2003;66:276–278. [PubMed: 12608865]
21. Barrero AF, Quilez Del Moral JF, Herrador MM. Studies in Natural Products Chemistry 2003;28:453–516. (Bioactive Natural Products (Part I)).
22. Macias FA, Simonet AM, Pacheco PC, Barrero AF, Cabrera E, Jimenez- Gonzalez D. J. Agric. Food Chem 2000;48:3003–3007. [PubMed: 10898656]
23. Barrero AF, Sanchez JF, Elmerabet J, Jimenez-Gonzalez D, Macias FA, Simonet AM. Tetrahedron 1999;55:7289–7304.
24. Barrero AF, Arseniyadis S, Quilez del Moral JF, Herrador MM, Valdivia M, Jimenez D. J. Org. Chem 2002;67:2501–2508. [PubMed: 11950294]
25. Hosoe T, Nozawa K, Lumley TC, Currah RS, Fukushima K, Takizawa K, Miyaji M, Kawai K-I. Chem. Pharm. Bull 1999;47:1591–1597. [PubMed: 10605057]
26. Singh P, Russell GB, Hayashi Y, Gallagher RT, Fredericksen S. Entomologia Experimentalis et Applicata 1979;25:121–127.
27. Kubo I, Matsumoto T, Klocke JA. J. Chem. Ecol 1984;10:547–559.
28. Zhang M, Ying BP, Kubo I. J. Nat. Prod 1992;55:1057–1062.
29. Hayashi Y, Kim Y, Hayashi Y, Chairul. Biosci., Biotechnol., Biochem 1992;56:1302–1303.
30. Barrero AF, Herrador MM, Quilez del Moral JF, Valdivia MV. Org. Lett 2002;4:1379–1382. [PubMed: 11950367]
31. Kubo I, Himejima M, Ying B-P. Phytochemistry 1991;30:1467–1469.
32. Adinolfi M, Mangoni L, Barone G, Laonigro G. Gazz. Chim. Ital 1973;103:1271–1279.
33. Michel A, Johnson RD, Duke SO, Scheffler BE. Environ. Toxicol. Chem 2004;23:1074–1079. [PubMed: 15095907]
34. Dayan FE, Romagni JG, Duke SO. J. Chem Ecol 2000;26:2079–2094.
35. Ritz, C.; Streibig, JC. J. Statist. Software. 2005. p. 1-22.http://www.bioassay.dk
36. Bharate SB, Khan SI, Yunus NAM, Chauthe SK, Jacob MR, Tekwani BL, Khan IA, Singh IP. Bioorg. Med. Chem 2007;15:87–96. [PubMed: 17070063]
37. Mustafa J, Khan SI, Ma G, Walker LA, Khan IA. Lipids 2004;39:167–172. [PubMed: 15134144]

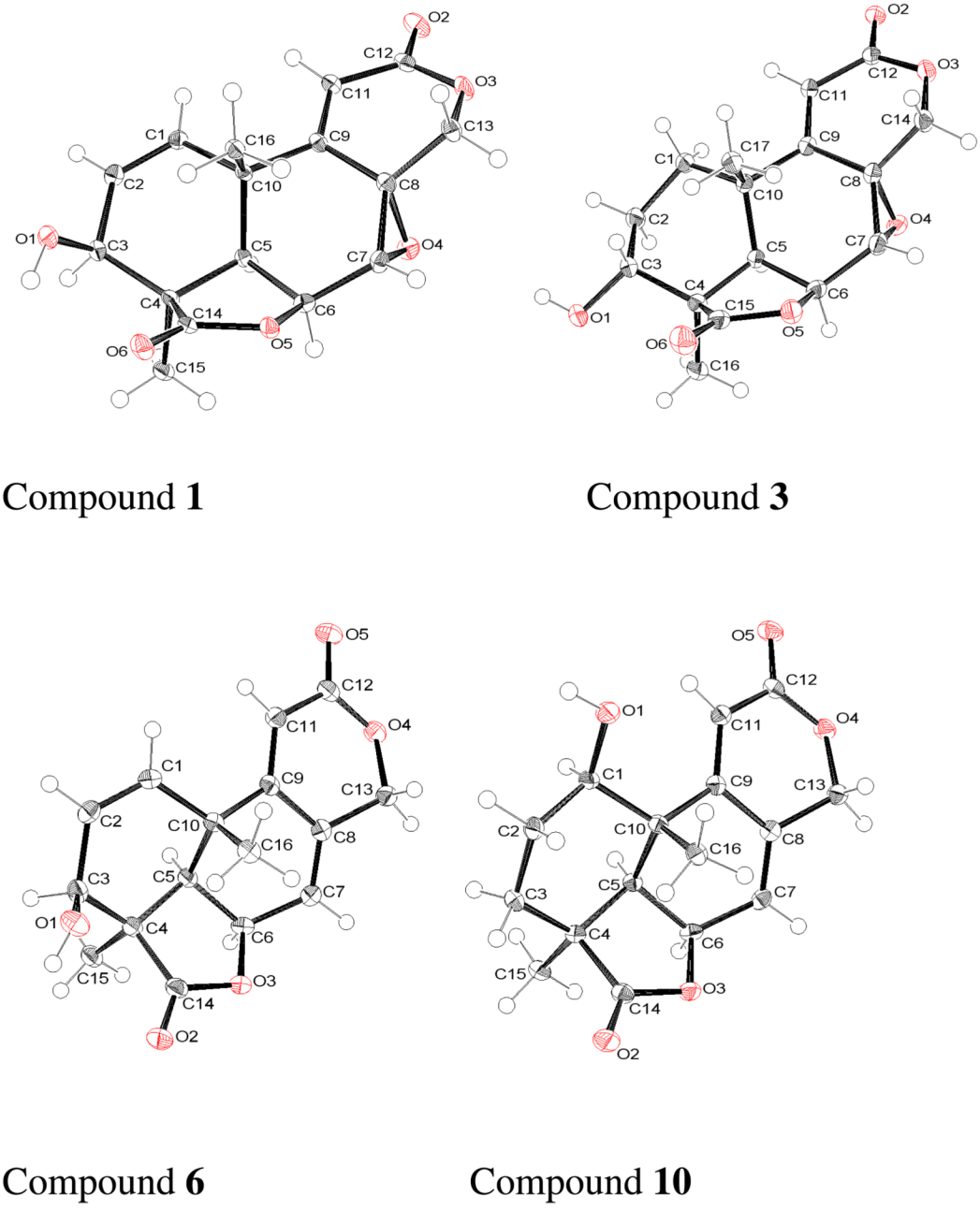

Figure 1.
Single-crystal X-ray structures of compounds 1, 3, 6, and 10.

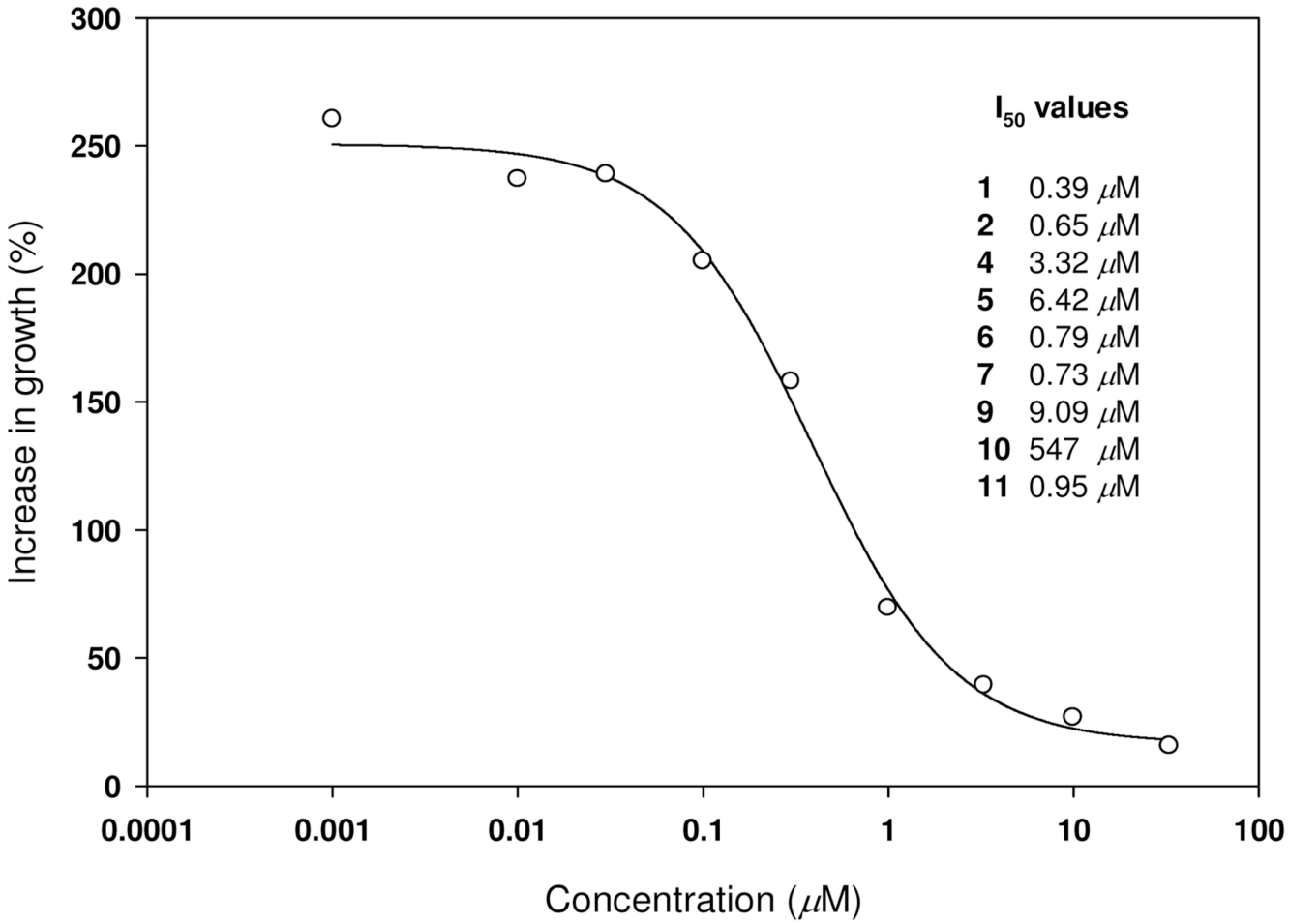

Figure 2.
Dose/response effect of **1** on growth of duckweed after seven days of exposure. Inset provides I_{50} values for **1** and the other most active compounds (Table 3) generated from dose/response data after seven days of exposure.

Table 1

^{1}H NMR Spectroscopic Data (400 MHz, $CDCl_3$/ CD_3OD) for Compounds **1**–**10**.

	1	2	3	4	5	6	7	8	9	10
Position				**δ_H (*J* in Hz)**						
1	6.37, d (10.0)	6.23, d (6.0)	1.68, m, 1.93, m	1.51, dd (13.5, 7.5) 2.32, dd (13.5, 9.0)	3.90, t (6.0)	6.61, d (9.6)	6.33, dd (9.6, 3.2)	1.66, m 1.83, m	1.34, dd (13.2, 7.2) 2.20, dd (13.6, 9.2)	3.78, t (6.4)
2	5.83, dd (10.0, 5.6)	5.90, ddd (6.8, 6.0, 2.0)	1.75, m, 1.89, m	3.94, m	1.63, m, 1.82, m	6.07, dd (10.0, 5.6)	5.90, ddd (9.6, 6.8, 2.4)	1.56, m 1.83, m	3.81, m	1.55, m, 1.76, m
3	4.16, d (5.6)	2.23, dd (18.8, 6.8) 2.79, d (18.8, 2.0)	4.25, dd (8.8, 3.2)	1.86, dd (13.5, 5.0) 2.05, dd (13.5, 12.5)	1.52, ddd (14.4, 8.4, 6.2), 2.24, ddd (14.0, 8.0, 5.6)	4.42, d (5.6)	2.83, ddd (18.0, 3.6, 2.4), 2.26, dd (18.0, 7.0)	4.31, dd (11.2, 4.0)	1.68, dd (13.6, 4.8) 1.96, t (13.2)	1.38, ddd, (14.4, 6.4, 6.4), 2.13, ddd (14.0, 8.0, 5.6)
5	2.02, d (4.8)	1.98, d (4.8)	2.05, d (4.8)	1.91, d (5.0)	1.81, d (4.4)	2.29, d (5.2)	2.08, d (4.6)	2.01, d (4.8)	1.81, d (5.2)	1.75, d (4.8)
6	4.74, d (4.4)	5.01, d (4.0)	5.08, dd (4.8, 1.2)	5.01, dd (5.0, 1.5)	4.96, dd (4.8, 1.2)	5.01, t, (5.0)	5.07, t (4.4)	4.94, brt (4.4)	4.89, td, (4,4, 1.2)	4.89, dt (4.8, 1.2)
7	3.81, d (1.2)	3.9, s	4.00, br.s	3.97, d (1.5)	3.92, br.s	6.24, m	6.25, m	6.10, m	6.08, m	6.05, m
11	6.08, s	6.23, s	6.00, s	6.04, s	6.56, s	6.00, d (1.6)	5.97, d (1.6)	5.71, br.s	5.62, d (1.6)	6.09, d (2.0)
13	3.97, d (12.8) 4.57, d (12.8)	4.13, d (12.4) 4.72, d (12.4)	4.12, d (12.8) 4.77, d (12.8)	4.12, d (12.4) 4.74, d (12.4)	4.07, d (12.4) 4.69, d (12.4)	4.91, d (13.6), 5.01, dt (14.0, 2.0)	4.89, d (13.2) 1.8), 4.99, dt (13.2, 2.0)	4.78, d (13.5) 4.85, brd (13.5)	4.73, d (14.0) 4.81, dt (13.6, 2.0)	4.70, d (13.5) 4.77, dt (13.5, 2.0)
15	1.23, s	1.34, s	1.30, s	1.36, s	1.23, s	1.49, s	1.38, s	1.22, s	1.21, s	1.11, s
16	1.26, s	1.12, s	1.17, s	1.25, s	1.14, s	1.47, s	1.14, s	1.05, s	1.06, s	0.98, s

Table 2

^{13}C NMR Spectroscopic Data (δ) (100 MHz, $CDCl_3/CD_3OD$) for Compounds **1**–**10**.

	1	**2**	**3**	**4**	**5**	**6**	**7**	**8**	**9**	**10**
position					**δ_C**					
1	133.6	128.7	27.7	39.1	68.9	135.1	130.1	28.6	36.5	69.1
2	129.4	127.7	26.7	63.5	29.2	129.5	127.4	26.1	64.2	29.2
3	69.5	31.8	65.7	36.7	27.6	69.6	31.3	65.1	39.8	27.0
4	46.3	43.0	48.1	41.9	42.3	47.3	43.6	48.6	43.1	42.8
5	48.5	45.0	43.5	41.9	43.8	52.7	49.2	48.0	46.3	47.8
6	72.2	73.6	72.3	72.6	72.6	71.7	72.6	72.2	72.4	71.6
7	53.3	53.5	53.4	53.2	53.6	122.4	122.2	121.9	122.5	122.1
8	55.6	55.4	55.4	54.7	60.0	132.6	132.3	131.8	132.2	132.6
9	154.4	154.4	159.0	158.1	156.3	155.8	155.1	159.0	159.4	157.6
10	37.2	37.0	35.6	36.5	40.9	36.9	36.5	34.4	36.3	40.2
11	117.4	117.9	117.1	118.1	120.2	111.7	111.9	111.9	112.6	113.8
12	163.1	162.6	164.1	163.3	164.3	164.8	163.6	164.3	165.1	165.1
13	72.2	72.0	72.3	72.0	72.3	69.9	69.7	69.7	70.3	69.9
14	178.9	181.6	181.2	181.3	181.2	179.6	181.9	182.1	182.4	181.4
15	24.5	25.0	15.9	22.5	23.6	25.0	25.4	15.9	23.4	23.9
16	28.4	24.9	27.2	29.1	17.8	26.8	22.9	26.9	27.9	16.7

Table 3

Antiplasmodial Activity of Compounds **1**–**13**

Compound	D6-clone		W2-clone		cytotoxicity
	IC_{50} ng/mL	S.I.	IC_{50} ng/mL	S. I.	IC_{50} ng/mL
1	750	2.0	600	2.5	1500
2	2300	>2.1	2300	>2.1	NC
3	NA	-	NA	-	NC
4	740	4.5	820	4.0	3300
5	NA	-	NA	-	NC
6	43	22.1	32	29.7	950
7	170	17.6	130	23.1	3000
8	NA	-	NA	-	NC
9	97	10.3	84	11.9	1000
10	900	5.3	670	7.1	4760
11	300	12.3	200	18.5	3700
12	250	6.8	190	8.9	1700
13	NA	-	NA	-	NC
chloroquine[a]	10		100		NC
artemisinin[a]	4.7		3.8		NC

[a]Positive controls

NC not cytotoxic at the highest dose (4760 ng/mL) tested

NA not active at the highest dose (4760 ng/mL) tested

S. I. (selectivity index) = IC50 for antiplasmodial activity/IC50 for cytotoxicity

Table 4

Cytotoxic Activity [IC_{50} (μg/mL)] of Compounds **1**–**13**

	SK-MEL	KB	BT-549	SK-OV-3	LLC-PK_{11}
1	0.58	4.4	4.8	8	2.8
2	2.8	NC	>10.0	NC	>10.0
3	NC	NC	NC	NC	NC
4	1.1	6.8	10.0	10.0	4.2
5	10	NC	NC	NC	NC
6	0.12	0.6	1.2	1.1	1.1
7	2.3	4.3	9.6	6.0	10.0
8	NC	NC	NC	NC	NC
9	0.41	2.1	4.7	3.2	1.2
10	3.3	>10.0	>10.0	>10.0	>10.0
11	1.1	4.2	>10.0	>10.0	5.4
12	0.72	4.5	9.0	6.3	4.8
13	NC	NC	NC	NC	NC
Doxorubicin [a]	0.6	0.9	1.3	0.6	0.6

[a] Positive control

NC = not cytotoxic up to highest test concentration of 10 μg/mL

Table 5

Phytotoxic Activity of Compounds **1**–**13**

Compound	Concentration (mg/mL)							
	1.0		0.1		0.01		0.001	
	L	B	L	B	L	B	L	B
1	5	5	5	5	5	4	2	2
2	5	5	5	5	3	4	0	1
3	5	5	4	4	0	0	0	0
4	5	5	5	5	3	2	0	0
5	5	5	5	5	4	4	1	0
6	5	5	5	5	5	4	0	0
7	5	5	5	5	1	3	0	0
8	5	5	2	3	0	0	0	0
9	5	5	5	5	2	3	1	2
10	5	5	5	5	1	1	0	0
11	5	5	5	5	2	3	0	0
12	5	5	4	4	2	1	0	0
13	1	0	0	0	0	0	0	0

L = lettuce; B = bentgrass

Ranking based on scale of 0 to 5

0 = no effect

5 = no growth